

# Millennial-scale climate cycles modulated by Milankovitch forcing in the middle Cambrian (ca. 500 Ma) Marjum Formation, Utah, USA

Damien Pas<sup>1,\*</sup>, Maya Elrick<sup>2</sup>, Anne-Christine Da Silva<sup>3</sup>, Linda Hinnov<sup>4</sup>, Valentin Jamart<sup>1</sup>, Marion Thauereau<sup>5</sup>, and Michiel Arts<sup>3</sup>

<sup>1</sup>Institute of Earth Sciences, University of Lausanne, 1015 Lausanne, Switzerland

<sup>2</sup>Earth and Planetary Sciences Department, University of New Mexico, Albuquerque, New Mexico 87131, USA

<sup>3</sup>Laboratoire de Pétrologie Sédimentaire, Département de Géologie, Université de Liège, 4000 Liège, Belgium

<sup>4</sup>Department of Atmospheric, Oceanic, and Earth Sciences, George Mason University, Fairfax, Virginia 22030, USA

<sup>5</sup>Natural History Museum, University of Oslo, 0562 Oslo, Norway

## ABSTRACT

Middle Cambrian offshore deposits of the Marjum Formation, Utah, USA, are characterized by four scales of superimposed cyclicity defined by varying fine siliciclastic versus limestone abundances; these include limestone-marl couplets (rhythmites; 5–10 cm), which are bundled into parasequences (1–2 m) and small-scale (5–10 m) and large-scale (20–40 m) sequences. Time series analysis of SiO<sub>2</sub> and lithologic rank stratigraphic series reveal cycles consistent with Milankovitch periods corresponding to Cambrian orbital eccentricity (20 m, 405 k.y.; 6 m, 110 k.y.), obliquity (1.8 m, 30 k.y.), climatic precession (1.15 m, 18 k.y.), and half-precession (0.64 m, 7 k.y.). Astronomical calibration of the lithologic rank series indicates that the main sub-Milankovitch cycle at 0.065 m represents ~1 k.y. and corresponds to the basic rhythmite couplet. All scales of cyclicity are interpreted as the result of wet versus dry monsoonal climate oscillations controlling the abundance of fine siliciclastic sediment influx to the basin. A plausible millennial-scale climate driver is solar activity. These results describe one of the oldest known geological candidates for solar-influenced climate change modulated by Milankovitch forcing.

## INTRODUCTION

Decades of deep-time (pre-Cenozoic) paleoclimate research reveal that the dominant building blocks of many Proterozoic through Phanerozoic marine and terrestrial sedimentary successions were generated by Milankovitch cycles (20–400 k.y.; Hinnov, 2013). Recognition of these persistent and widespread sedimentary cycles provides important insights into Earth's climate history, and such cycles provide the basis for high-resolution refinement of the geologic time scale (Hinnov, 2018; Huang, 2018; Westerhold et al., 2020; Wu et al., 2023).

In some depositional settings with high sedimentation rates and limited bioturbation (lakes, glacial ice, speleothems), sub-Milankovitch-scale cyclicity is preserved, offering high-reso-

lution climate histories and chronometers (Neff et al., 2001; Nederbragt and Thurow, 2005; Steinhilber et al., 2012; Misra et al., 2020). However, these settings are geographically and temporally limited; their climate records are challenging to apply in global studies, across geologically long time intervals, or in assessing potential relationships with concurrent Milankovitch-scale climate drivers.


By contrast, offshore settings of epicontinental seas typical of the Paleozoic–Mesozoic eras are geographically widespread and geologically long lived, and have relatively high sedimentation rates that can potentially capture millennial-scale events. Indeed, millennial-scale cyclicity is well documented in many offshore deposits, commonly expressed as strikingly rhythmic interbeds of thin limestone and shale or marl rhythmite (Garrison and Fischer, 1969; Elrick and Hinnov, 2007; Franco et al., 2012). Rhythmites have developed across a wide range of climatic, tectonic, bio-

logic, eustatic, and seawater chemistry conditions and are typically explained as the result of millennial-scale wet versus dry climatic oscillations (Elrick and Hinnov, 2007). Many reports documenting millennial-scale cyclicity in Phanerozoic marine and terrestrial records (e.g., Anderson, 2011; Kochhann et al., 2020; Boulila et al., 2022) have interpreted that this scale of climate variability was externally driven and thus a permanent feature of the Earth ocean-atmosphere system; however, each system needs to be assessed individually to ascertain the validity of such interpretations.

Stratigraphic and geochemical data sets collected from the middle Cambrian Marjum Formation, Utah, USA, indicate that millennial-scale climate variability forced the development of the centimeter-scale rhythmite that form the building blocks of superimposed cycles. This study describes four scales of cyclicity in the Marjum Formation, estimates the cycle durations, and discusses potential cycle origins and relationships among the interpreted paleoclimate drivers.

## GEOLOGICAL BACKGROUND

During the Cambrian, Laurentia was positioned in the southern paleo-tropics; its paleo-western margin accumulated thick upper Proterozoic–Devonian passive-margin deposits (see Supplemental Material<sup>1</sup>). In the middle Cambrian, the House Range embayment study area accumulated deep- then shallow-marine deposits (Fig. 1A). The Marjum Formation (Drumian; 504.5 Ma to 500.5 Ma; Peng et al., 2020) offshore deposits are composed of four superimposed scales of sedimentary cycles (Fig. 1; Elrick and Snider, 2002; Brett et al. 2009):

Damien Pas  <https://orcid.org/0000-0002-2235-1974>  
\*damien.pas@unil.ch

<sup>1</sup>Supplemental Material. Methods, depositional model, Figures S1–S6, time series analysis scripts and data. Please visit <https://doi.org/10.1130/GEOL.S.25760934> to access the supplemental material; contact [editing@geosociety.org](mailto:editing@geosociety.org) with any questions.

CITATION: Pas, D., et al., 2024, Millennial-scale climate cycles modulated by Milankovitch forcing in the middle Cambrian (ca. 500 Ma) Marjum Formation, Utah, USA: *Geology*, v. XX, p. , <https://doi.org/10.1130/G52182.1>

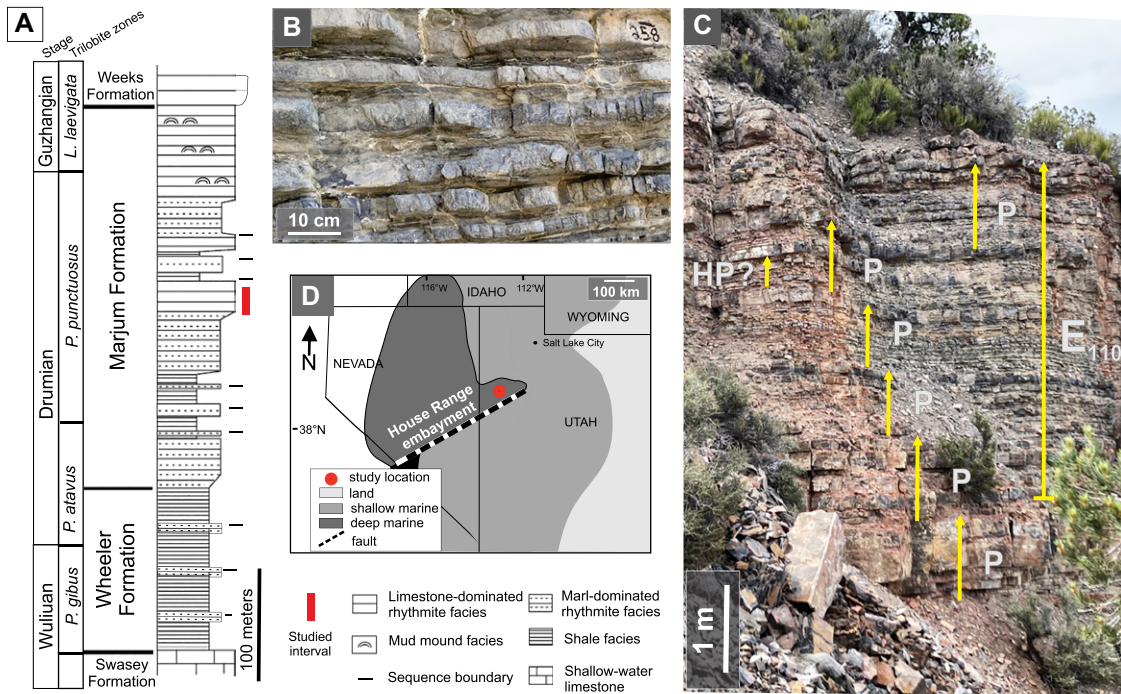


**Figure 1.** (A) Cambrian stratigraphy at Marjum Pass, House Range, Utah, USA (from Elrick and Snider, 2002). (B) Details of typical limestone-dominated rhythmites. (C) Field photograph of a portion of the studied Marjum Formation showing stacked rhythmites, potential half-precession (HP?), precession (P), and short eccentricity ( $E_{110}$ ; see details in Fig. S6 [see text footnote 1]). (D) Cambrian paleogeography of the western USA showing the location of the study area within the House Range embayment (Foster and Gaines, 2016). *L*—*Lejopyge*; *P*—*Ptychagnostus*.

large-scale sequences (20–40 m), small-scale sequences (5–10 m), parasequences (1–2 m), and limestone-marl rhythmites (5–10 cm). All cycle scales are defined by systematic variations in fine siliciclastic versus limestone content (see Supplemental Material).

## RESULTS

### Lithologic Cyclicity

In the study interval, 517 limestone (lime mudstone)–marl couplets were identified, most ranging in thickness from 3 to 7 cm (median 5 cm; Fig. S1 in the Supplemental Material). Couplets vary from marl dominated (marl layers  $>2\times$  the thickness of adjacent limestone layers), to limestone and marl layers of similar thicknesses, to limestone dominated (limestone layers  $>2\times$  the thickness of adjacent marl layers). The syn-sedimentary origin (versus diagenetic origin; Munnecke and Samtleben, 1996) of the limestone-marl couplets is supported by preserved sedimentary structures and trace fossils in both types of layers (for details, see Elrick and Hinnov, 1996, 2007).

Parasequences (1–2 m) occur throughout the Marjum Formation and are defined by repeated successions of limestone-dominated couplets at parasequence bases, overlain by marl-dominated couplets, and capped by limestone-dominated couplets or a limestone bed ( $\sim 20$  cm) lacking marl interbeds (Fig. 1C; Fig. S6; Elrick and Snider, 2002). Small-scale sequences (5–10 m) are identified by similar patterns as those for parasequences but at a thicker scale, i.e., stacked limestone-dominated parasequences followed by marl-dominated parasequences, returning to limestone-dominated parasequences (Fig. 1C).

Large-scale sequences (20–40 m) are identified by variations in marl content, with marl-rich intervals weathering to slopes and limestone-rich intervals forming cliffs; this lithologic cyclicity is observed throughout the Marjum and underlying Wheeler Formations (Fig. 1; Langenburg, 2003; Brett et al., 2009).

### Time Series Analysis

Chemostratigraphic profiles for typical detrital proxies ( $\text{SiO}_2$ ,  $\text{TiO}_2$ ,  $\text{Fe}_2\text{O}_3$ ,  $\text{K}_2\text{O}$ ) show increased abundances aligning with marl-rich intervals, indicating that these proxies faithfully track variations in terrigenous input (Fig. S2). The  $\text{SiO}_2$  stratigraphic series, with its enhanced variability, reveals high spectral power at 20 m, 5.8 m, 1.8 m, 1.15 m, 0.64 m, and 0.3 m in continuous wavelet transform (CWT) analysis (Fig. 2A). The 10 cm sampling resolution does not permit confident interpretation of cycles thinner than 0.4 m (Martinez et al., 2016). CWT analysis of the lithologic rank series shows the presence of peaks at 20 m, 5.8 m, and 1.15 m alongside a prominent 0.065 m peak (Fig. 2).

Modulation of couplet thicknesses was assessed by filtering out the median couplet thickness and applying spectral analysis on its Hilbert transform (Fig. S3). The power spectrum shows two main amplitude modulation frequencies at 0.0097 cycles/cm (560 cm) and 0.0017 cycles/cm (105 cm) wavelengths. Bandpass filters centered on the main periodicities observed in both  $\text{SiO}_2$  and rank series are shown to visualize the relationship between changes in  $\text{SiO}_2$ –rank series and potential astronomical cycles. Code and data are available in the Supplemental Material.

## DISCUSSION

### Cycle Durations

The CWT spectral peaks in the  $\text{SiO}_2$  stratigraphic series have similar ratios to calculated Cambrian Milankovitch periods (Fig. 2A; Waltham, 2015). These results suggest that the 20 m, 5.8 m, 1.8 m, 1.15 m, and 0.64 m peaks correspond to long orbital eccentricity (405 k.y.), short orbital eccentricity (110 k.y.), obliquity (30 k.y.), climatic precession (18.5 k.y.), and half-precession (7 k.y.), respectively, which is supported by integrated biostratigraphic and sediment accumulation rate (SAR) constraints (Fig. 2; Supplemental Material). CWT analysis of the lithologic rank series shows ratios similar to those expected for long and short orbital eccentricity and climatic precession, suggesting that the systematic variation of limestone versus marl layer thicknesses was modulated by Milankovitch forcing. The lack of a 1.8 m cycle in the lithologic rank series compared with the X-ray fluorescence–measured  $\text{SiO}_2$  series is presumably because the latter is more sensitive than subjective field observations of lithologic changes.

The relationship between marl- versus limestone-dominated intervals is explicit when plotting the short orbital eccentricity filter output against the stratigraphy (Fig. 2B). This supports the interpretation that parasequences identified by field observations of varying rhythmite types and the lithologic rank series represent precession-driven (and possibly also obliquity-driven) sedimentary cycles and that the small-scale sequences represent a short orbital eccentricity signal. Although we can identify only portions of two large-scale sequences in the stratigraphy,

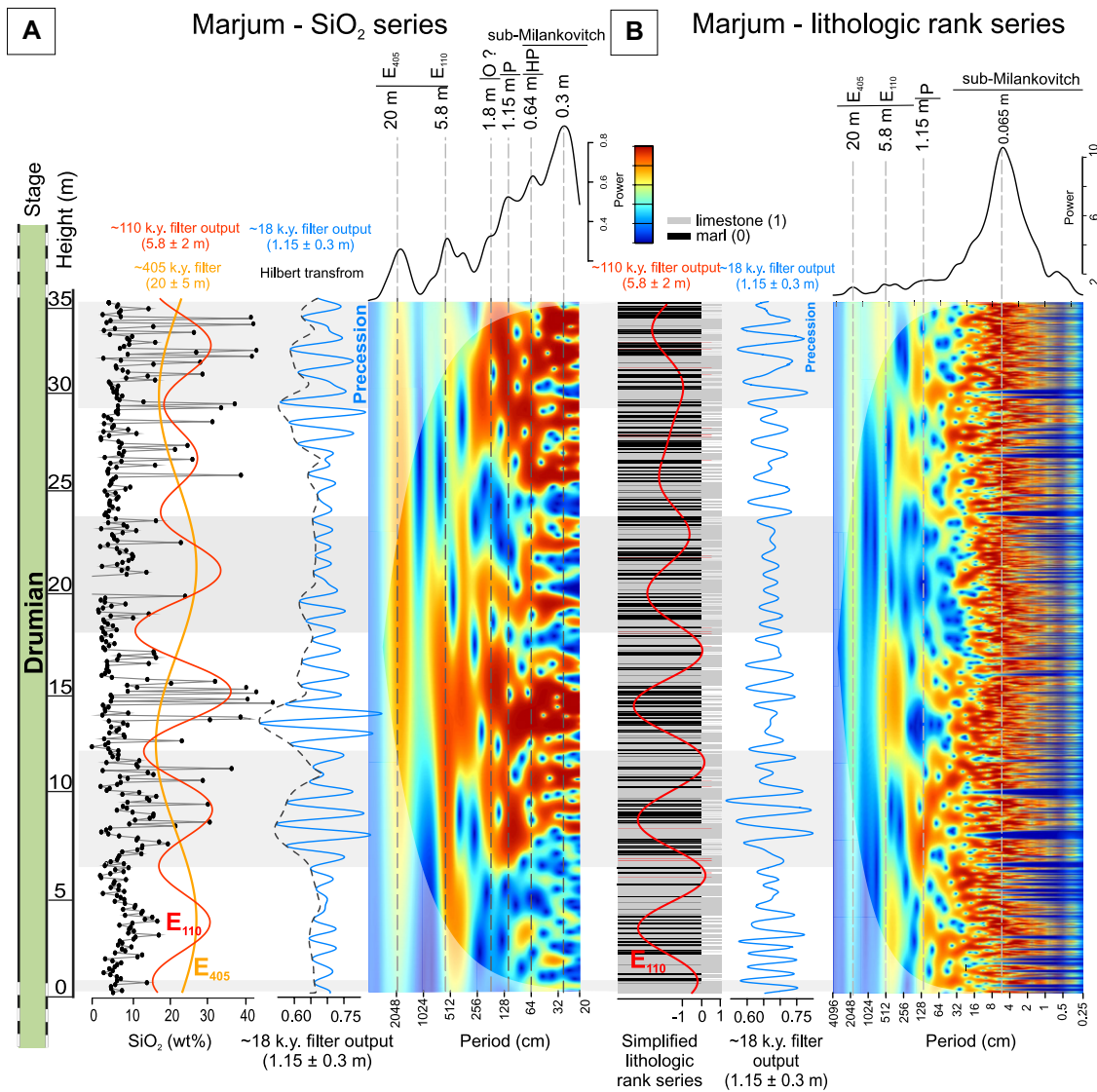


**Figure 2.** (A) Left:  $\text{SiO}_2$  stratigraphic series with interpreted 405 k.y. (long eccentricity,  $E_{405}$ ; orange line), 110 k.y. (short eccentricity,  $E_{110}$ ; red line), and 18 k.y. (blue line) Taner-filtered output series. Hilbert transform of the precession band is shown as black dashed line. (Astrochron R package; Meyers, 2014). Right: Continuous wavelet transform (CWT) analysis (Arts, 2023) with corresponding peak power at 20 m, 5.8 m, 1.15 m, and 0.3 m. O—obliquity; P—precession; HP—half-precession. (B) Left: Lithologic rank stratigraphic series with 110 k.y. (red line) and 18 k.y. (blue line) Taner-filtered output series. Right: CWT analysis with the corresponding peak power at 20 m, 5.8 m, 1.15 m, and 0.065 m. Horizontal gray shaded areas are meant to help visualize common trends.

the occurrence of a 20 m cycle in the  $\text{SiO}_2$  and lithologic rank power spectra may represent a long orbital eccentricity signal.

Assuming that Milankovitch cycles influenced parasequence and sequence formation, we use the interpreted short orbital eccentricity period (110 k.y.) to calibrate the  $\text{SiO}_2$  and the lithologic rank series (Fig. S5). The  $\text{SiO}_2$  series indicates a 668.75 k.y. duration, and the lithologic rank series represents 680 k.y.; the temporal similarity between the two independent data sets strengthens the Milankovitch forcing interpretation and provides an estimated average SAR of 5.25 cm/k.y. for the study interval, similar to previous studies of the Marjum Formation (Elrick and Hinnov, 2007). Using this SAR, the median ~5-cm-thick couplets represent 0.95 k.y., and the average 6.5-cm-thick couplets represent ~1.2 k.y. Importantly, this average ~1 k.y. duration for couplets is consistent with the occurrence of 16–19 rhythmite composing each climatic precession–forced parasequence (Fig. S6). The astronomically calibrated records

reveal distinct peak power corresponding to long and short (calibrated) orbital eccentricity and elevated power at obliquity and climatic precession periods, which would be expected when tuning to a single astronomical frequency (“minimal tuning”; Muller and MacDonald, 2000). High power in sub-Milankovitch bands at 7 k.y., 3 k.y., and 1 k.y. is recorded in the lithologic rank series (Fig. S5).

### Cycle Origins

The millennial-scale rhythmite is the primary building blocks of all scales of Marjum Formation cyclicity. Changes in siliciclastic content are attributed to millennial-scale climate oscillations, with relatively wet conditions associated with increased continental weathering and transport of siliciclastics to offshore settings followed by relatively dry climates with increased limestone accumulation. In our depositional model in the Supplemental Material, rhythmite couplets are considered “dilution” cycles (see De Vleeschouwer et al. [2024] for a

review of the different origins of marl–limestone alternation).

Similar climatic interpretations have been made for other Phanerozoic marine and terrestrial successions (Nederbragt and Thurow, 2005; Franco et al., 2012; Kochhann et al., 2020). Holocene ice cores, deep-sea sediment cores, tree rings, and speleothem records suggest that solar activity cycles in the range of Eddy cycle periodicity (~900–1050 yr; Scafetta and Bianchini, 2022) influenced monsoon intensity, based on a strong correlation between speleothem or ice  $\delta^{18}\text{O}$  (precipitation) and tree ring  $\Delta^{14}\text{C}$  (solar activity; Stuiver et al., 1998). The Eddy solar cycle offers a possible explanation for the ~1 k.y. couplet cycle. Although variations in solar irradiance are small, modeling indicates that oceanic and atmospheric responses can amplify the climatic impact globally (e.g., Riechelson et al., 2023).

The 3 k.y.  $\text{SiO}_2$  peak could be attributed to the Hallstatt solar cycle (~2100–2500 yr). Similar periodicities of ~2.4 k.y. are reported

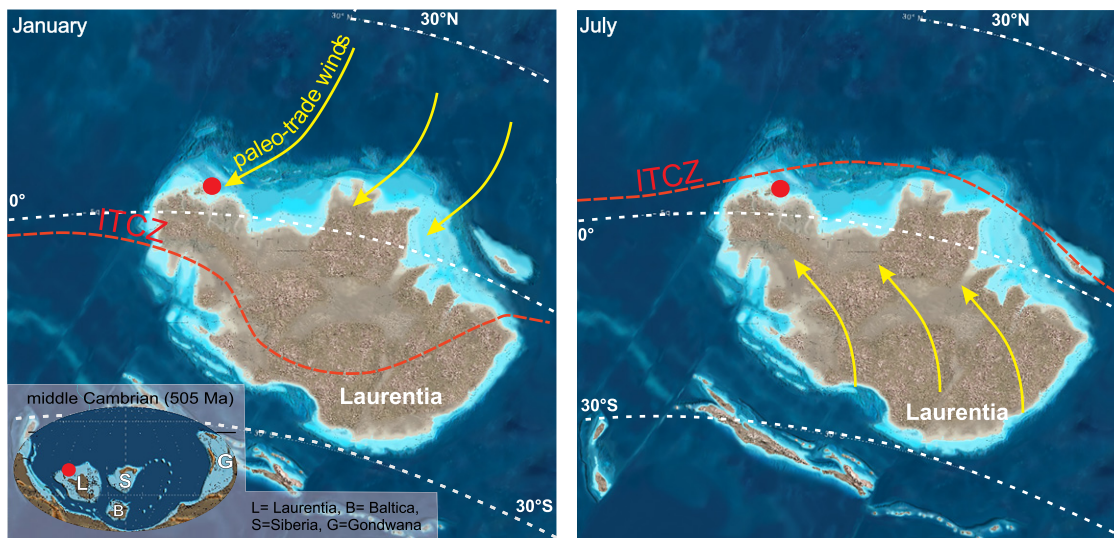


**Figure 3. Conceptual model showing the interpreted seasonal shifts of the middle Cambrian Intertropical Convergence Zone (ITCZ) (red dashed line). Red dot shows location of the study area. Paleogeographic maps ©2023 Colorado Plateau Geosystems Inc. Used with permission.**

from Lower Devonian (Da Silva et al., 2018) and Permian marine (Franco et al., 2012) and restricted marine records (Anderson, 2011). The 7 k.y. spectral peak falls in the range of the half-precession cycle, which is related to the twice-annual migration of the Intertropical Convergence Zone (ITCZ) over the equator (Fig. 3). The paleotropical position of the study area and a similar half-precession signal in the lower Cambrian of South China (Zhang et al., 2022) supports this interpretation. The lithologic rank time series lacks both the 3 k.y. (15 cm) and 7 k.y. (64 cm) peaks, and the reasons for their absence remain unclear.

The parasequences are interpreted as the result of Milankovitch-forced variations in monsoon-related wet versus dry climates and eustatic sea-level changes and are considered both carbonate “transport” (or carbonate productivity) and “dilution” cycles (see the Supplemental Material). Limestone-dominated couplets at the base of a parasequence reflect drier millennial-scale climate cycles (and rising sea level), followed by marl-dominated couplets representing wetter phases (highstand), and finally, at the top, a return to drier climates (and falling or lowstand sea levels) and limestone-dominated couplets. Small-scale sequences, formed by stacked successions of limestone- versus marl-dominated parasequences, mirror changes in monsoon intensity and sea level attributed to short orbital eccentricity. Large-scale sequences (20 m, 405 k.y.) are not entirely resolved in the study interval (which only spans ~680 k.y.), but they have been observed previously in the Marjum Formation (Elrick and Snider, 2002), Wheeler Formation (Langenburg, 2003; Brett et al., 2009), and coeval shallow-marine deposits across western Laurentia (Bond et al., 1991; Montañez and Osleger, 1993) and have been interpreted as Milankovitch-forced sea-level variations based on interpreted water-depth fluctuations and facies stacking patterns. Sea-

level variations occurred in tandem with climate change: high sea levels align with wetter climates and deeper-water facies rich in siliciclastics, while low sea levels align with drier climates and shallower-water facies characterized by limestone-dominated facies.

In sum, all scales of cyclicity of the Marjum Formation are interpreted as the result of dry versus wet climate oscillations from monsoons forced by solar activity at millennial time scales and modulated by Milankovitch forcing. During the Cambrian, the combination of a tropical paleolatitude and the large continental area of Laurentia strengthened monsoonal intensity at both time scales, driven by the migration dynamics of the ITCZ (Fig. 3).

## CONCLUSIONS

Four scales of stratigraphic cyclicity are observed in the middle Cambrian (Drumian) Marjum Formation of western Laurentia: limestone-marl couplets (5–10 cm) bundled into parasequences (1–2 m) and small-scale (5–10 m) and large-scale (20 m) sequences. All cycle scales are defined by variations in fine siliciclastics versus limestone. Time series analysis of a 35.5-m-long SiO<sub>2</sub> stratigraphic series (detrital proxy) and a lithologic rank stratigraphic series based on field observations reveals peak power consistent with Cambrian long orbital eccentricity (20 m, 405 k.y.), short orbital eccentricity (6 m, 110 k.y.), obliquity (1.8 m, 30 k.y.), climatic precession (1.15 m, 18 k.y.), and half-precession (0.64 m, 7 k.y.). The main spectral power in the lithologic rank series occurs at a 0.065 m wavelength representing ~1 k.y. (millennial) couplets. Stratigraphic data combined with spectral analysis supports the interpretation that both millennial and Milankovitch cycles were controlled by wet versus dry monsoonal climate oscillations influencing siliciclastic influx to the marine basin. A plausible millennial-scale climate driver for the centimeter-scale couplets is solar activity related

to Eddy and Hallstatt solar cycles. These results provide one of the oldest known records of solar-influenced climate change and support the idea that solar activity and Milankovitch forcing are permanent features affecting paleoclimate variability.

## ACKNOWLEDGMENTS

D. Pas acknowledges the Swiss National Sciences Foundation grant PZ00P2-193520. L. Hinnov was partially supported by Heising Simons Foundation grant 2021-2796. A.C. Da Silva is thankful for the Fonds de la Recherche Scientifique grants J.0037.21, T.0051.19, T.0037.22, and R.5541-J-F-B. This is a contribution to UNESCO Project IGCP 652. Grant T.0051.19 supported M. Arts. We are grateful to Sebastien Wouters for field assistance. We thank Kathleen Benison for her editorial work, and David De Vleeschouwer and two anonymous reviewers for their thoughtful reviews.

## REFERENCES CITED

- Anderson, R.Y., 2011, Enhanced climate variability in the tropics: A 200 000 yr annual record of monsoon variability from Pangea's equator: *Climate of the Past*, v. 7, p. 757–770, <https://doi.org/10.5194/cp-7-757-2011>.
- Arts, M., 2023, WaverideR: Extracting signals from wavelet spectra: <https://cran.r-project.org/package=WaverideR> (accessed January 2024/).
- Bond, G.C., Kominz, M.A., and Beavan, J., 1991, Evidence for orbital forcing of Middle Cambrian peritidal cycles: Wah Wah range, south-central Utah, in Franseen, E.K., et al., eds., *Sedimentary Modeling—Computer Simulations and Methods for Improved Parameter Definition*: Kansas Geological Survey Bulletin 233, p. 293–317.
- Boulila, S., Galbrun, B., Gardin, S., and Pellenard, P., 2022, A Jurassic record encodes an analogous Dansgaard-Oeschger climate periodicity: *Scientific Reports*, v. 12, 1968, <https://doi.org/10.1038/s41598-022-05716-8>; correction available at <https://doi.org/10.1038/s41598-022-08065-8>.
- Brett, C.E., Allison, P.A., DeSantis, M.K., Liddell, W.D., and Kramer, A., 2009, Sequence stratigraphy, cyclic facies, and *lagerstätten* in the Middle Cambrian Wheeler and Marjum Formations, Great Basin, Utah: *Palaeogeography, Palaeoclimatology, Palaeoecology*, v. 277, p. 9–33, <https://doi.org/10.1016/j.palaeo.2009.02.010>.
- Da Silva, A.C., Dekkers, M.J., De Vleeschouwer, D., Hladil, J., Chadimova, L., Slavik, L., and Hilgen,

- F.J., 2018, Millennial-scale climate changes manifest Milankovitch combination tones and Hallstatt solar cycles in the Devonian greenhouse world: *Geology*, v. 47, p. 19–22, <https://doi.org/10.1130/G45511.1>.
- De Vleeschouwer, D., Percival, L.M.E., Wichern, N.M.A., and Batenburg, S.J., 2024, Pre-Cenozoic cyclostratigraphy and palaeoclimate responses to astronomical forcing: *Nature Reviews Earth & Environment*, v. 5, p. 59–74, <https://doi.org/10.1038/s43017-023-00505-x>.
- Elrick, M., and Hinnov, L.A., 1996, Millennial-scale climate origins for stratification in Cambrian and Devonian deep-water rhythmites, western USA: *Palaeogeography, Palaeoclimatology, Palaeoecology*, v. 123, p. 353–372, [https://doi.org/10.1016/0031-0182\(95\)00106-9](https://doi.org/10.1016/0031-0182(95)00106-9).
- Elrick, M., and Hinnov, L.A., 2007, Millennial-scale paleoclimate cycles recorded in widespread Palaeozoic deeper water rhythmites of North America: *Palaeogeography, Palaeoclimatology, Palaeoecology*, v. 243, p. 348–372, <https://doi.org/10.1016/j.palaeo.2006.08.008>.
- Elrick, M., and Snider, A.C., 2002, Deep-water stratigraphic cyclicity and carbonate mud mound development in the Middle Cambrian Marjum Formation, House Range, Utah, USA: *Sedimentology*, v. 49, p. 1021–1047, <https://doi.org/10.1046/j.1365-3091.2002.00488.x>.
- Foster, J.R., and Gaines, R.R., 2016, Taphonomy and paleoecology of the “Middle” Cambrian (Series 3) formations in Utah’s West Desert: Recent finds and new data, *in* Comer, J.B., et al., eds., *Resources and Geology of Utah’s West Desert*: Utah Geological Association Publication 45, p. 291–336.
- Franco, D.R., Hinnov, L.A., and Ernesto, M., 2012, Millennial-scale climate cycles in Permian–Carboniferous rhythmites: Permanent feature throughout geologic time?: *Geology*, v. 40, p. 19–22, <https://doi.org/10.1130/G32338.1>.
- Garrison, R.E., and Fischer, A.G., 1969, Deep-water limestones and radiolarites of the Alpine Jurassic, *in* Friedman, G.M., ed., *Depositional Environments in Carbonate Rocks*: SEPM (Society for Sedimentary Geology) Special Publication 14, p. 20–54, <https://doi.org/10.2110/pec.69.03.0020>.
- Hinnov, L.A., 2013, Cyclostratigraphy and its revolutionizing applications in the earth and planetary sciences: *Geological Society of America Bulletin*, v. 125, p. 1703–1734, <https://doi.org/10.1130/B30934.1>.
- Hinnov, L.A., 2018, Cyclostratigraphy and astrochronology in 2018, *in* Montenari, M., ed., *Stratigraphy & Timescales, Volume 3: Cyclostratigraphy and Astrochronology*: New York, Academic Press, p. 1–80, <https://doi.org/10.1016/bs.sats.2018.08.004>.
- Huang, C., 2018, Astronomical time scale for the Mesozoic, *in* Montenari, M., ed., *Stratigraphy & Timescales, Volume 3: Cyclostratigraphy and Astrochronology*: New York, Academic Press, p. 81–150, <https://doi.org/10.1016/bs.sats.2018.08.005>.
- Kochhann, M.V.L., Cagliari, J., Kochhann, K.G.D., and Franco, D.R., 2020, Orbital and millennial-scale cycles paced climate variability during the Late Paleozoic Ice Age in the southwestern Gondwana: *Geochemistry, Geophysics, Geosystems*, v. 21, <https://doi.org/10.1029/2019GC008676>.
- Langenburg, E.S., 2003, The Middle Cambrian Wheeler Formation: Sequence stratigraphy and geochemistry across a ramp-to-basin transition [M.S. thesis]: Logan, Utah State University, 133 p., <https://doi.org/10.26076/0f21-5c8b>.
- Martinez, M., Kotov, S., De Vleeschouwer, D., Pas, D., and Pällike, H., 2016, Testing the impact of stratigraphic uncertainty on spectral analyses of sedimentary series: *Climate of the Past*, v. 12, p. 1765–1783, <https://doi.org/10.5194/cp-12-1765-2016>.
- Meyers, S., 2014, Astrochron: An R Package for Astrochronology: <https://cran.r-project.org/web/packages/astrochron/index.html> (accessed January 2024).
- Misra, P., Farooqui, A., Sinha, R., Khanolkar, S., and Tandon, S.K., 2020, Millennial-scale vegetation and climatic changes from an Early to Mid-Holocene lacustrine archive in Central Ganga Plains using multiple biotic proxies: *Quaternary Science Reviews*, v. 243, <https://doi.org/10.1016/j.quascirev.2020.106474>.
- Montañez, I.P., and Osleger, D.A., 1993, Parasequence stacking patterns, third-order accommodation events, and sequence stratigraphy of Middle to Upper Cambrian platform carbonates, Bonanza King Formation, southern Great Basin, *in* Loucks, R.G., and Sarg, J.F., eds., *Carbonate Sequence Stratigraphy: Recent Developments and Applications*: American Association of Petroleum Geologists Memoir 57, p. 305–326, <https://doi.org/10.1306/M57579C12>.
- Muller, R.A., and MacDonald, G.J., 2000, Ice Ages and Astronomical Causes: Data, Spectral Analyses and Mechanisms: Chichester, UK, Springer-Praxis, 318 p.
- Munnecke, A., and Samtleben, C., 1996, The formation of micritic limestones and the development of limestone-marl alternations in the Silurian of Gotland, Sweden: *Facies*, v. 34, p. 159–176, <https://doi.org/10.1007/BF02546162>.
- Nederbragt, A.J., and Thurow, J., 2005, Geographic coherence of millennial-scale climate cycles during the Holocene: *Palaeogeography, Palaeoclimatology, Palaeoecology*, v. 221, p. 313–324, <https://doi.org/10.1016/j.palaeo.2005.03.002>.
- Neff, U., Burns, S.J., Mangini, A., Mudelsee, M., Fleitmann, D., and Matter, A., 2001, Strong coherence between solar variability and the monsoon in Oman between 9 and 6 kyr ago: *Nature*, v. 411, p. 290–293, <https://doi.org/10.1038/35077048>.
- Peng, S.C., Babcock, L.E., and Ahlberg, P., 2020, The Cambrian Period, *in* Gradstein, F.M., et al., eds., *Geologic Time Scale 2020*: Amsterdam, Elsevier, p. 565–629, <https://doi.org/10.1016/B978-0-12-824360-2.00019-X>.
- Riechelton, H., Bova, S.C., Rosenthal, Y., Meyers, S., and Bu, K., 2023, Solar cycles forced Southern Westerly Wind migrations during the Holocene: *Geophysical Research Letters*, v. 50, <https://doi.org/10.1029/2023GL104148>.
- Scafetta, N., and Bianchini, A., 2022, The planetary theory of solar activity variability: A review: *Frontiers in Astronomy and Space Sciences*, v. 9, <https://doi.org/10.3389/fspas.2022.937930>.
- Steinhilber, F., et al., 2012, 9,400 years of cosmic radiation and solar activity from ice cores and tree rings: *Proceedings of the National Academy of Sciences of the United States of America*, v. 109, p. 5967–5971, <https://doi.org/10.1073/pnas.1118965109>.
- Stuiver, M., Reimer, P.J., Bard, E., Beck, J.W., Burr, G.S., Hughen, K.A., Kromer, B., McCormac, G., Van Der Plicht, J., and Spurk, M., 1998, INTCAL98 radiocarbon age calibration, 24,000–0 cal BP: *Radiocarbon*, v. 40, p. 1041–1083, <https://doi.org/10.1017/S0033822200019123>.
- Waltham, D., 2015, Milankovitch period uncertainties and their impact on cyclostratigraphy: *Journal of Sedimentary Research*, v. 85, p. 990–998, <https://doi.org/10.2110/jsr.2015.66>.
- Westerhold, T., et al., 2020, An astronomically dated record of Earth’s climate and its predictability over the last 66 million years: *Science*, v. 369, p. 1383–1387, <https://doi.org/10.1126/science.aba6853>.
- Wu, H., Fang, Q., Hinnov, L.A., Zhang, S., Yang, T., Shi, M., and Li, H., 2023, Astronomical time scale for the Paleozoic Era: *Earth-Science Reviews*, v. 244, <https://doi.org/10.1016/j.earscirev.2023.104510>.
- Zhang, T., Li, Y., Fan, T., Da Silva, A.-C., Shi, J., Gao, Q., Kuang, M., Liu, W., Gao, Z., and Li, M., 2022, Orbitally-paced climate change in the early Cambrian and its implications for the history of the Solar System: *Earth and Planetary Science Letters*, v. 583, <https://doi.org/10.1016/j.epsl.2022.117420>.

Printed in the USA